A Non-linear Dynamics Approach to Classify Gait Signals of Patients with Parkinson's Disease

P. A. Pérez-Toro[1*], J. C. Vásquez-Correa[1,2], T. Arias-Vergara[1,2], N. Garcia-Ospina[1], J. R. Orozco-Arroyave[1,2], and E. Nöth[2]

[1]Faculty of Engineering, University of Antioquia UdeA, Medellín, Colombia.
[2]University of Erlangen-Nüremberg, Germany.
paula.perezt@udea.edu.co

Abstract. Parkinson's disease is a neuro-degenerative disorder characterized by different motor symptoms, including several gait impairments. Gait analysis is a suitable tool to support the diagnosis and to monitor the state of the disease. This study proposes the use of non-linear dynamics features extracted from gait signals obtained from inertial sensors for the automatic detection of the disease. We classify two groups of healthy controls (Elderly and Young) and Parkinson's patients with several classifiers. Accuracies ranging from 86% to 92% are obtained, depending on the age of the healthy control subjects.

Key words: Parkinson's disease, Gait assessment, Inertial sensors, Non-linear dynamics, Classification

1 Introduction

Parkinson's disease (PD) is a neuro-degenerative disorder characterized by the progressive loss of dopaminergic neurons in the mid brain [1], which produces motor and non-motor impairments. Motor symptoms include lack of coordination, tremor, rigidity, and postural instability. Gait impairments appear in most of patients and include freezing, shuffling, and festinating gait. The standard scale to evaluate the neurological state of the patients is the Movement Disorder Society-Unified Parkinson's Disease Rating Scale (MDS-UPDRS-III) [2]. The third section of the scale contains 14 items to evaluate the lower limbs.

Gait analysis of PD patients have been performed commonly with inertial sensors e.g., accelerometers and gyroscopes attached to the shoes of the patients [3, 4]. Several studies have described gait impairments of PD patients using kinematics features related to the speed and length of each stride, which are computed from signals captured from the inertial sensors. In [5] several inertial sensors attached to the lower and upper limbs were used to predict the neurological state of PD patients. The authors computed features related to stance time, length of the stride, and velocity of each step, and reported a Pearson's correlation coefficient of 0.60 between predicted values and real UPDRS score. In [6] the authors classified PD patients and healthy control (HC) subjects with kinematic

features computed from inertial sensors attached to the shoes. The features include the stride time, the swing phase, the heel force, the stride length, and others. The authors reported accuracies of up to 90% using a classifier based on Linear discriminant analysis. Recently in [7] the authors proposed new features to assess gait impairments in PD patients. Those new features were the peak forward acceleration in the loading phase and peak vertical acceleration around heel-strike, which encode the engagement in stride initiation and the hardness of the impact at heel-strike, respectively. The results indicated that the proposed features correlate with the disease progression and the loss of postural agility/stability of the patients. In previous studies [8] we computed kinematics features from gait signals captured with the same inertial sensors [9] to evaluate the neurological state of the patients. A Spearman's correlation of up to 0.72 was reported between the MDS-UPDRS-III score of the patients and the predicted values obtained with a support vector regressor.

Although the success of the kinematics features to assess the gait symptoms of PD patients, there are components related with the stability during the walking process that cannot be characterized properly with the classical approach. In order to model those components it is necessary to use Nonlinear dynamics (NLD) features [10, 11]. This study considers several NLD features to model the gait process of PD patients and HC subjects. The features include correlation dimension (CD), Largest Lyapunov exponent (LLE), Hurst exponent (HE), Lempel-Ziv Complexity (LZC), and several entropy measures, which have proved to be suitable for the NLD analysis of PD [11, 12]. Three classifiers are considered: K-Nearest Neighbors (KNN), Support Vector Machine (SVM) and Random Forest (RF). As aging is an interesting aspect that deserves attention, its effect is considered by the inclusion of two groups of HC subjects: Young HC subjects (YHC) and elderly HC (EHC). The results confirmed that age is an important factor that needs to be addressed when patients with neurodegenerative diseases are considered. In addition, we reported accuracies ranging from 86% to 92%, depending on the age of the HC subjects.

2 Data

Gait signals were captured with the eGaIT system[1], which consists of a 3D-accelerometer (range ±6g) and a 3D gyroscope (range ±500°/s) attached to the lateral heel of the shoes [4]. Figure 1 shows the eGait system and the inertial sensor attached to the lateral heel of the shoe. The signals are transmitted by bluetooth to a tablet where they are received by an android app.

Data from both foot were captured with a sampling rate of 100 Hz and 12-bit resolution. The tasks performed by the patients include 20 meters walking with a stop at 10 meters (Two times 10 m walk, 2x10m), and 40 meters walking with a stop every 10 meters (Four times 10 m walk, 4x10m).

Data are obtained from 45 PD patients and 89 HC subjects. The HC subjects were divided into two groups: the first one formed with 44 YHC (Young

[1] Embedded Gait analysis using Intelligent Technology, `http://www.egait.de/`

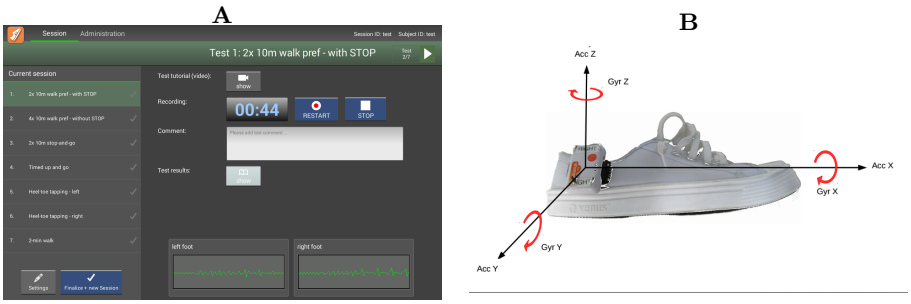

Fig. 1: Interface eGaiT and shoe with its attached inertial sensor.

Healthy Controls), and the second one with 45 EHC (Elderly Healthy Controls) subjects. The patients were evaluated by an expert neurologist and labeled according to the MDS-UPDRS-III score. Table 1 shows additional information of the participants of this study.

Table 1: General information of the subjects. **PD** patients: Parkinson's disease patients. **HC**: healthy controls. $\boldsymbol{\mu}$: average. $\boldsymbol{\sigma}$: standard deviation. **T**: disease duration.

	PD patients		YHC subjects		EHC subjects	
	male	female	male	female	male	female
Number of subjects	17	28	26	18	23	22
Age ($\mu \pm \sigma$)	65 ± 10.3	58.9 ± 11.0	25.3 ± 4.8	22.8 ± 3.0	66.3 ± 11.5	59.0 ± 9.8
Range of age	41-82	29-75	21-42	19-32	49-84	50-74
T ($\mu \pm \sigma$)	9 ± 4.6	12.6 ± 12.2				
Range of duration of the disease	2-15	0-44				
MDS-UPDRS-III ($\mu \pm \sigma$)	37.6 ± 21.0	33 ± 20.3				
Range of MDS-UPDRS-III	8-82	9-106				

3 Methods

3.1 Nonlinear Dynamics Feature extraction

Phase Space. The phase space reconstruction is the first step for the NLD analysis. The Takens's Theorem [13] is used for such a purpose. The phase space is represented by Equation 1 for a time-series s_t. The time-delay τ is computed by the first minimum of the mutual information function, and the embedding dimension m is found using the false neighbor method [14].

$$\boldsymbol{S_t} = \{s_t, s_{t-\tau}, ...s_{t-(m-1)\tau}\} \tag{1}$$

Figure 2 shows the phase space obtained from gait signals considering 20 meters walking with a stop at 10 meters from three subjects: (A) YHC, (B)

EHC, and (C) PD patient. Note that the phase space for the YHC exhibits well defined trajectories and a clear recurrence, conversely the trajectories of PD patient attractor are scattered. Several NLD features can be computed from the phase space to assess the complexity and stability of the walking process.

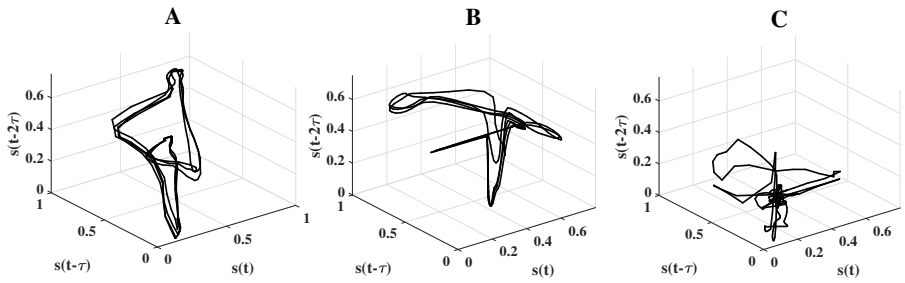

Fig. 2: Phase space from gait signals from 20 meters walking with a stop at 10 meters of . (A) Female YHC with 22 years old. (B) Female EHC with 52 years old. (C) Female PD patient with 52 years old and MDS-UPDRS=49.

Correlation Dimension(CD) establishes a measure over the exact space that is occupied by the phase space. The correlation sum $C(\epsilon)$ is defined for a set of points x_n of the phase space according to Equation 2. Where θ is the Heaviside step function. $C(\epsilon)$ counts the distance between x_i and x_j that are lower than a threshold ϵ and N is the number of embedded points. To compute the CD, a linear regression of $\ln(C(\epsilon))$ vs $\ln(\epsilon)$ is performed. The slope of the resultant line for a small ϵ value corresponds to CD [15].

$$C(\epsilon) = \lim_{n\to\infty} \frac{1}{N(N-1)} \sum_{i=1}^{N} \sum_{j=i+1}^{N} \theta(\epsilon - |x_i - x_j|) \tag{2}$$

Largest Lyapunov Exponent (LLE) measures the sensitivity to initial conditions of the signal, and gives information about the stability properties of the gait signal. LLE quantifies the exponential divergence of the neighbor paths in a phase space, i.e., it measures the degree of non-periodicity of a given signal. After the reconstruction of the phase-space, the nearest neighbor of each embedded point is located. LLE is estimated as the mean separation rate between the nearest neighbor, according to $d(t) = Ae^{\lambda t}$, where λ corresponds to the LLE, $d(t)$ is the mean divergence in an instant t and A is a constant for normalization [15].

Hurst Exponent (HE) evaluates the long-term dependency of the time series. The HE is a smoothness measure of a fractal time series based on an asymptotic

behavior of the re-scaled range of the signal. The HE is computed by $T^{\mathrm{HE}} = \frac{R}{S}$, T is the duration of time-series and $\frac{R}{S}$ corresponds to the re-scaled range [15].

Lempel-Ziv complexity (LZC) correlates the number of different patterns that lie along a sequence. It reflects the order that is retained in a one-dimensional temporal pattern of symbols. The signal is transformed into binary sequences according to the difference between consecutive samples, and the LZC reflects the rate of new patterns in the sequence, and ranges from 0 (deterministic sequence) to 1 (random sequence) [16].

Entropy Measures Six entropy measurements are computed: One of them corresponds to the Approximate Entropy (ApEn), which provides a general regularity measure. After computing the correlation sum C_i defined by Equation 2, we define an average version according to Equation 3. m is the pattern length and r is the effective filter. ApEn is defined as the increment of $\phi^m(r)$ between two immediate steps of m, i.e., $\mathrm{ApEn}(m, r, N) = \phi^m(r) - \phi^{m+1}(r)$.

$$\phi^m(r) = \frac{1}{N-m+1} \sum_{i=1}^{N-m+1} \log C_i^m(r) \tag{3}$$

Each point in the phase space counts itself when we compute the ApEn. ApEn depends on the length of the time series, causing that short gait signals have a lower estimation than the expected. To avoid this problems the Sample Entropy (SampEn) [17] is also considered in this study. The regularity of the signals computed with ApEn and SampEn is affected by the discontinuity of the Heaviside function in Equation 2. A proposed solution [18] consists of replacing the Heaviside step function with a Gaussian kernel in the estimation of $C_i^m(r)$. We compute the ApEn and the SampEn with the Gaussian kernel functions.

Another measure considered to analyze the deterministic and chaotic dynamics of gait signals is the Recurrence Probability Density Entropy (RPDE), which is computed using the close returns algorithm [19]. Let's assume there is a small circle $B(S_{n0}, r)$ with radius $r > 0$, which is located close to the data embedded point S_{n0}. Then, the time instant n_1, where the first orbit returns to the circle, is recorded. The difference between two time instants is the recurrence time $T = n_1 - n_0$. The process is repeated for all embedded points S_n, forming an histogram of recurrence times $R(T)$. RPDE is computed according to Equation 4, where T_{max} is the maximum recurrence time.

$$\mathrm{RPDE} = -\frac{R(i)\ln(R(i))}{\ln(T_{max})} \tag{4}$$

To compute the stochastic component of the walking process, the Detrended Fluctuation Analysis (DFA) is considered. DFA allows to obtain long-term dependencies of the time-series similar to the HE, except that DFA may be applied to time-series whose underlying statistics are non-stationary.

The above features were extracted from over the entire gait signal. Table 2 shows the number of computed features for each task performed by the patients. Ten NLD features are extracted, which are computed for each of the six signals from the inertial sensors, forming the feature matrix used to classify PD patients and HC subjects.

Table 2: Number of features per task

Foot	Task	Number of axes	Number of features	Total
Left	2x10m	6	10	60
Left	4x10m	6	10	60
Left	Fusion	6	20	120
Right	2x10m	6	10	60
Right	4x10m	6	10	60
Right	Fusion	6	20	120
Both	2x10m	12	10	120
Both	4x10m	12	10	120
Both	Fusion	12	20	240

3.2 Classification

Three classifiers are considered: KNN, SVM with Gaussian kernel, and RF. We ran a 5-fold cross validation, where 3 folds were used for training, one for validation and one for test respectively. The optimization criterion is based on the accuracy on the validation set. The parameter were optimized in a grid search over the train folds, as follows: $\mathbf{K} \in \{3, 5, ...11\}$ for KNN, $\mathbf{C}$ and $\boldsymbol{\gamma} \in \{10^{-4}, 10^{-3}, ...10^{4}\}$ for SVM and number of trees ($\mathbf{N}$) $\in \{5, 10, 20, 30, 50, 100\}$ and depth of the decision tress ($\mathbf{D}$) $\in \{2, 5, 10, 20, 30, 50, 100\}$ for RF.

4 Experiments and results

Two experiments are performed: (1) classification of PD vs. YHC , and (2) classification of PD vs. EHC. Individual experiments are performed by foot and per task. In addition, the features computed from the two tasks and feet are combined. Table 3 shows the results for the PD vs. YHC subjects. In general the best results are obtained with the RF classifier. The fusion of features from both feet and the two tasks also provides the highest accuracy (91.0%±4.9).

The average accuracy in train for table 3 for the tree classifiers was respectively, KNN=88.3%±2.7, SVM=95.4%±4.0 and RF=99.1%±1.8.

Although the high accuracies of the experiment classifying PD vs. YHC subjects, it does not consider the effect of age in the walking process. The results classifying PD patients vs. EHC subjects with similar age to the patients are shown in Table 4. Note that the results are slightly lower than those obtained

Table 3: Results to classify PD patients vs. YHC subjects. **ACC:** accuracy in the test set, **AUC:** Area under ROC curve, **K:** number of neighbors in the KNN. **C and γ:** complexity parameter and bandwidth of the kernel in the SVM, **N and D:** Number of trees and depth of the decision trees in the RF.

		KNN				SVM					RF				
Foot	**Task**	**ACC(%) ($\mu \pm \sigma$)**	**Sen(%)/Spe(%)**	**AUC**	**K**	**ACC(%)**	**Sen(%)/Spe(%)**	**AUC**	**C**	γ	**ACC(%)**	**Sen(%)/Spe(%)**	**AUC**	**N**	**D**
Left	2x10	85.4%±6.4	75.6/95.3	0.91	5	82.0%±5.0	75.6/88.6	0.92	10^1	10^{-3}	86.5%±7.6	80.0/93.3	0.92	20	20
Left	4x10	84.4%±8.1	73.3/95.6	0.95	9	91.1%±6.3	86.7/95.6	0.96	10^0	10^{-3}	93.3%±7.2	93.3/93.3	0.94	30	20
Left	Fusion	88.8%±3.8	77.8/100.0	0.94	5	88.9%±8.8	82.2/95.6	0.94	10^1	10^{-3}	91.1%±7.4	86.7/95.6	0.95	20	100
Right	2x10	85.5%±4.8	71.1/100.0	0.88	9	79.9%±8.3	77.8/81.9	0.91	10^1	10^{-3}	82.0%±4.6	77.8/86.1	0.92	10	5
Right	4x10	78.8%±9.0	60.0/97.8	0.90	7	92.2%±4.9	84.4/100.0	0.92	10^1	10^{-3}	86.6%±6.2	84.4/88.9	0.95	10	100
Right	Fusion	82.1%±9.0	68.9/95.6	0.91	7	88.8%±4.9	80.0/61.8	0.93	10^1	10^{-3}	89.9%±6.2	84.4/95.6	0.95	50	5
Both	2x10	86.7%±5.0	73.3/97.8	0.93	7	83.2%±6.7	80.0/86.7	0.94	10^1	10^{-3}	85.5%±11.5	80.0/91.1	0.92	5	2
Both	4x10	84.2%±10.7	71.1/97.8	0.93	5	86.6%±4.8	80.0/93.3	0.90	10^0	10^{-3}	92.2%±6.3	88.9/95.6	0.94	20	2
Both	Fusion	86.5%±2.9	73.3/100.0	0.93	5	91.0%±4.9	84.4/97.8	0.96	10^0	10^{-3}	91.1%±4.9	84.4/97.8	0.96	30	10
Average		**84.7**	**71.6/97.7**	**0.92**	–	**87.1**	**81.2/89.0**	**0.93**	–	–	**88.7**	**84.4/92.9**	**0.94**	–	–
STD		**2.7**	**5.1/2.0**	**0.0**	–	**4.2**	**3.5/11.6**	**0.0**	–	–	**3.5**	**4.8/3.7**	**0.0**	–	–

in the previous experiment. Although such an impact, relatively high acuracies are obtained, specially when we combine the features from both tasks and both feet. For the separate classification using features computed from each foot, the highest accuracies are obtained for the left foot, which may indicate that the left lower limbs are more affected due to the disease, having in mind that most of the patients are right dominant foot. This fact is known as cross laterality [20].

Table 4: Results to classify PD patients vs. EHC subjects. **ACC:** accuracy in the test set, **AUC:** Area under ROC curve, **K:** number of neighbors in the KNN. **C and γ:** complexity parameter and bandwidth of the kernel in the SVM, **N and D:** Number of trees and depth of the decision trees in the RF.

		KNN				SVM					RF				
Foot	**Task**	**ACC(%)**	**Sen(%)/Spe(%)**	**AUC**	**K**	**ACC(%)**	**Sen(%)/Spe(%)**	**AUC**	**C**	γ	**ACC(%)**	**Sen(%)/Spe(%)**	**AUC**	**N**	**D**
Left	2x10	81.1±9.3	80.0/82.2	0.84	5	77.78±13.0	66.7/88.9	0.74	10^{-4}	10^{-4}	83.3±14.2	73.3/93.3	0.89	30	2
Left	4x10	72.2±11.1	68.9/75.6	0.80	5	81.11±12.8	86.7/75.6	0.90	10^0	10^{-3}	84.4±7.2	82.2/86.7	0.89	10	5
Left	Fusion	80.0±8.4	73.3/86.7	0.86	5	83.33±6.8	82.2/84.4	0.84	10^{-4}	10^{-4}	83.3±8.8	77.8/88.9	0.89	30	30
Right	2x10	70.0±9.3	60.0/80.0	0.82	5	67.78±7.2	51.1/84.4	0.73	10^{-4}	10^{-4}	78.9±6.1	73.3/84.4	0.79	10	2
Right	4x10	77.8±6.8	73.3/82.2	0.82	3	76.67±7.2	73.3/80.0	0.83	10^1	10^{-3}	80.0±11.5	80.0/80.0	0.87	20	2
Right	Fusion	81.1±8.4	73.3/88.9	0.85	3	82.22±4.6	75.6/88.9	0.87	10^1	10^{-3}	85.6±6.3	82.2/88.9	0.91	20	5
Both	2x10	76.7±12.7	68.9/84.4	0.79	5	80.00±8.4	68.9/91.1	0.85	10^1	10^{-4}	78.9±11.4	71.1/86.7	0.86	30	50
Both	4x10	72.2±3.9	75.6/68.9	0.80	3	81.11±6.3	77.8/84.4	0.83	10^{-4}	10^{-4}	82.2±12.7	82.2/82.2	0.91	100	50
Both	Fusion	85.6±5.0	77.8/93.3	0.89	3	82.22±4.6	71.1/93.3	0.86	10^{-4}	10^{-4}	85.6±2.5	80.0/91.1	0.91	30	30
Average		**77.4**	**72.3/82.5**	**0.83**	–	**79.14**	**72.6/85.7**	**0.83**	–	–	**82.3**	**78.0/86.9**	**0.88**	–	–
STD		**4.8**	**5.8/7.2**	**0.0**	–	**4.5**	**10.25/5.6**	**0.1**	–	–	**2.4**	**4.4/4.2**	**0.0**	–	–

The average accuracy in train for table 4 for the tree classifiers was respectively, KNN=87.8%±4.3, SVM=91.4%±5.9 and RF=97.9%±3.1.

Figure 3 shows an additional comparison among the best results obtained in the classification of PD patients vs. the two groups of HC subjects. The ROC curves represent the results in a more compact way and it is a standard measure of performance in medical applications. The three classifiers produce similar results for both experiments. The impact of age in the results is also observed.

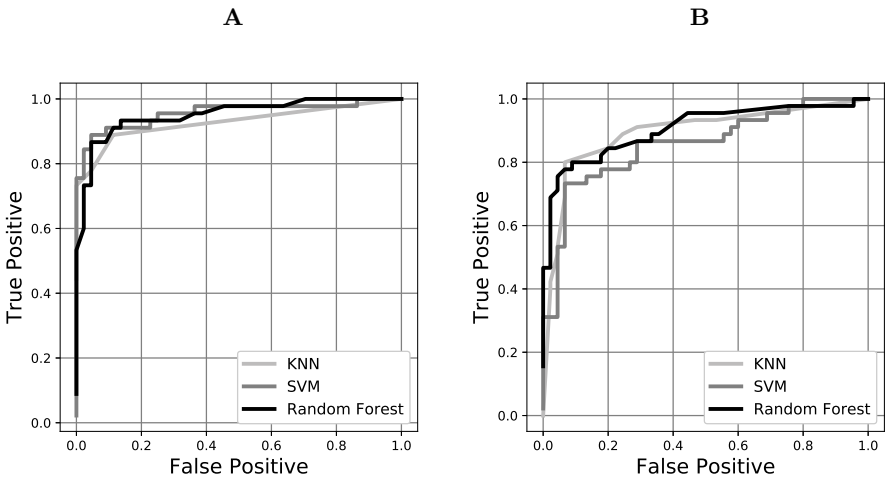

Fig. 3: ROC curve graphics of the best results. A) PD vs YHC. B) PD vs EHC. In both cases the fusion of features from both feet and both tasks are considered.

In addition, Figures (4, 5 and 6) show the scores of each classifier. In KNN and RF, the score is the probability with which sample belongs to the selected class and in SVM is the distance of the hyperplane to the sample.

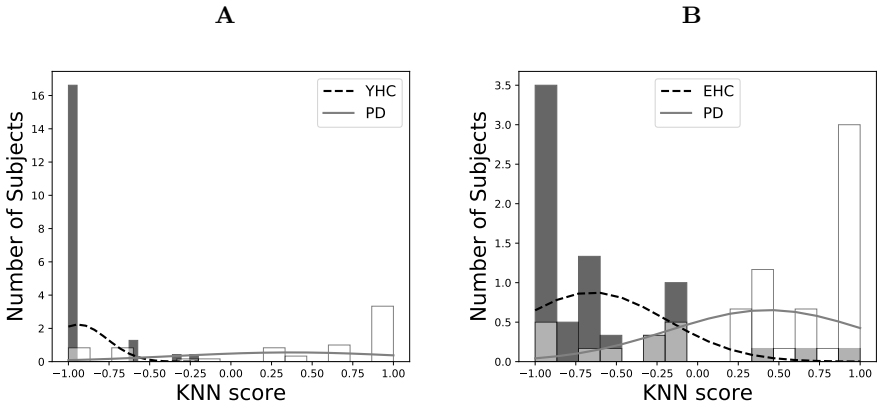

Fig. 4: KNN Scores of Fusion Both Feet task. A) PD vs YHC. B) PD vs EHC.

In figure 4.A is observed that YHC subjects are correctly classified, which corresponds to a specificity of 100.0% for this task in table 3, while in PD patients, the sensitivity is lower (73.3%), playing the age factor an important role. Respect to the figure 4.B, is obtained a lower specificity, because similar

age between both populations, and it tends to get confused between patients and elderly healthy controls.

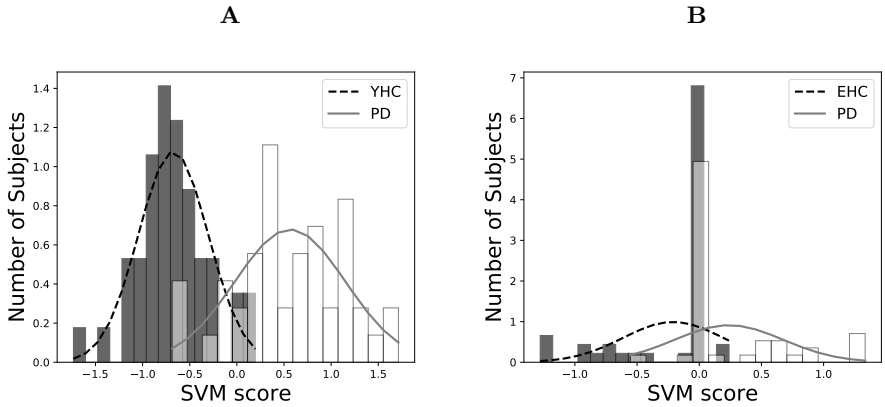

Fig. 5: SVM Scores of Fusion Both Feet task. A) PD vs YHC. B) PD vs EHC.

In figure 5. A higher maximization of the hyperplane in comparison with the figure 5.B can be observed with bigger distances values than in PD vs. EHC being the elderly healthy controls very close to the patients, agreeing also with the higher accuracies (table 3) in the classification of PD vs. YHC.

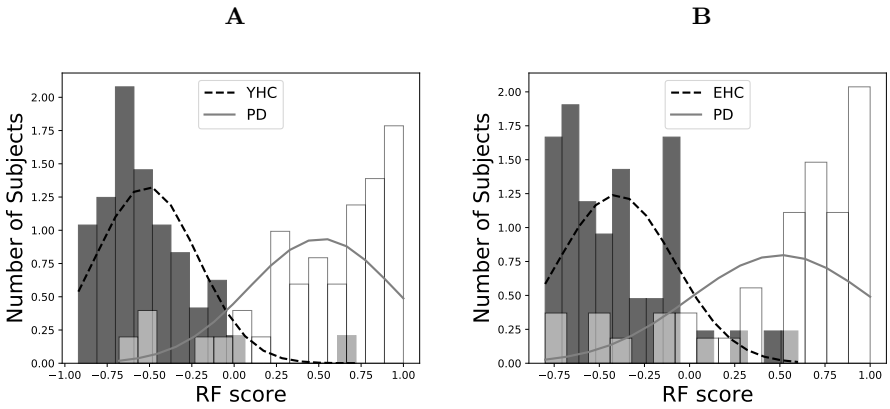

Fig. 6: RF Scores of Fusion Both Feet task. A) PD vs YHC. B) PD vs EHC.

According to the figure 6 a larger separability between the histograms is observed in PD vs. YHC, being easier to classify considering the big difference between the average age (Table 1). In figure 6.B patients are miss-classified with elderly controls.

Any of the methods is able to find patterns that discriminate to the controls, however, many PD patients are in an early stage of the disease, where the motor capabilities are not too affected yet.

5 Conclusion

An automatic assessment of gait of PD patients is proposed in this study. A NLD approach is considered to evaluate stability, long-term dependency, and complexity of the walking process of the patients. An automatic discrimination between PD patients and two groups of HC subjects is performed to assess the impact of age in the walking process. The set of NLD features included features computed from the phase space and several entropy measures.

The combination of features extracted from different tasks and from both feet is more effective in the classification process, i.e., both tasks and feet provide complementary information to discriminate between PD patients and HC subjects. The results also indicate the presence of the cross laterality effect [20], since higher accuracies are obtained classifying the features computed from the left foot rather than those computed from the right foot, although most of the subjects from this study are right-handed. Further experiments will consider the evaluation of the neurological state of the patients by classifying patients in several stages of the disease according to the MDS-UPDRS-III score. Other NLD based features can also be considered. The proposed features might also be combined with standard kinematics features to improve the results.

Acknowledgments

This work was financed by CODI from University of Antioquia grant #2015–7683. This project has received funding from the European Union's Horizon 2020 research and innovation programme under the Marie Sklodowska-Curie Grant Agreement No. 766287.

References

1. Hornykiewicz, O.: Biochemical aspects of Parkinson's disease. Neurology **51**(2 Suppl 2) (1998) S2–S9
2. Goetz C. G., et al.: Movement Disorder Society-sponsored revision of the Unified Parkinson's Disease Rating Scale (MDS-UPDRS): Scale presentation and clinimetric testing results. Movement Disorders **23**(15) (2008) 2129–2170
3. Oung, Q.W., Muthusamy, H., et al.: Technologies for assessment of motor disorders in Parkinson's disease: a review. Sensors **15**(9) (2015) 21710–21745
4. Klucken, J., Barth, J., et al.: Unbiased and mobile gait analysis detects motor impairment in Parkinson's disease. PloS one **8**(2) (2013) e56956
5. Parisi, F., Ferrari, G., et al.: Body-sensor-network-based kinematic characterization and comparative outlook of UPDRS scoring in leg agility, sit-to-stand, and gait tasks in Parkinson's disease. IEEE Journal of Biomedical and Health Informatics **19**(6) (2015) 1777–1793

6. Perumal, S.V., Sankar, R.: Gait and tremor assessment for patients with parkinson's disease using wearable sensors. ICT Express **2**(4) (2016) 168–174
7. Hannink, J., Gaßner, H., et al.: Inertial sensor-based estimation of peak accelerations during heel-strike and loading as markers of impaired gait patterns in PD patients. Basal Ganglia **8** (2017) 1
8. Vasquez-Correa, J.C., et al.: Multi-view representation learning via gcca for multimodal analysis of parkinson's disease. In: International Conference on Acoustics, Speech and Signal Processing (ICASSP). (2017) 2966–2970
9. Pérez-Toro, P.A., Vásquez-Correa, J.C., et al.: Análisis motriz en las extremidades inferiores para el monitoreo del estado neurológico de pacientes con enfermedad de parkinson. In: Symposium on Signal Processing, Images and Artificial Vision (STSIVA). (2016)
10. Dingwell, J.B., Cusumano, J.P.: Nonlinear time series analysis of normal and pathological human walking. Chaos: An Interdisciplinary Journal of Nonlinear Science **10**(4) (2000) 848–863
11. Sejdic, E., et al.: A comprehensive assessment of gait accelerometry signals in time, frequency and time-frequency domains. IEEE Transactions on Neural Systems and Rehabilitation Engineering **22**(3) (2014) 603–612
12. Orozco-Arroyave, J.R., et al.: Analysis of speech from people with parkinson's disease through nonlinear dynamics. In: International Conference on Nonlinear Speech Processing, Springer (2013) 112–119
13. Takens, F.: On the numerical determination of the dimension of an attractor. Lecture notes in mathematics **1125**(11) (1985) 99–106
14. Kennel, M.B., et al.: Determining embedding dimension for phase-space reconstruction using a geometrical construction. Physical review A **45**(6) (1992) 3403
15. Kantz, H., Schreiber, T.: Nonlinear time series analysis. Volume 7. Cambridge university press (2004)
16. Lempel, A., Ziv, J.: On the complexity of finite sequences. IEEE Transactions on Information Theory **22**(1) (1976) 75–81
17. Richman, J.S., Moorman, J.R.: Physiological time-series analysis using approximate entropy and sample entropy. American Journal of Physiology-Heart and Circulatory Physiology **278**(6) (2000) H2039–H2049
18. Xu, L.S., et al.: Gaussian kernel approximate entropy algorithm for analyzing irregularity of time-series. In: International Conference on Machine Learning and Cybernetics. (2005) 5605–5608
19. Lathrop, D.P., Kostelich, E.J.: Characterization of an experimental strange attractor by periodic orbits. Physical Review A **40**(7) (1989) 4028
20. Sadeghi, H., Allard, P., Prince, F., Labelle, H.: Symmetry and limb dominance in able-bodied gait: a review. Gait & posture **12**(1) (2000) 34–45